



Ultrafast Charge Separation in Bilayer WS₂/Graphene Heterostructure Revealed by Time- and Angle-Resolved Photoemission Spectroscopy

Razvan Krause^{1,2*}, Mariana Chávez-Cervantes², Sven Aeschlimann^{1,2}, Stiven Forti³, Filippo Fabbri^{3,4,5}, Antonio Rossi^{3,4}, Camilla Coletti^{3,5}, Cephise Cacho⁶, Yu Zhang⁷, Paulina Ewa Majchrzak⁸, Richard T. Chapman⁷, Emma Springate⁷ and Isabella Gierz^{1*}

OPEN ACCESS

Edited by:

Gang Zhang,
Institute of High Performance
Computing, Agency for Science,
Technology and Research (A*STAR),
Singapore

Reviewed by:

Yuriy Dedkov,
Shanghai University, China
David R. Heskett,
University of Rhode Island,
United States

*Correspondence:

Razvan Krause
razvan.krause@ur.de
Isabella Gierz
isabella.gierz@ur.de

Specialty section:

This article was submitted to
Condensed Matter Physics,
a section of the journal
Frontiers in Physics

Received: 15 February 2021

Accepted: 23 March 2021

Published: 29 April 2021

Citation:

Krause R, Chávez-Cervantes M,
Aeschlimann S, Forti S, Fabbri F,
Rossi A, Coletti C, Cacho C, Zhang Y,
Majchrzak PE, Chapman RT,
Springate E and Gierz I (2021)
Ultrafast Charge Separation in Bilayer
WS₂/Graphene Heterostructure
Revealed by Time- and
Angle-Resolved Photoemission
Spectroscopy. *Front. Phys.* 9:668149.
doi: 10.3389/fphy.2021.668149

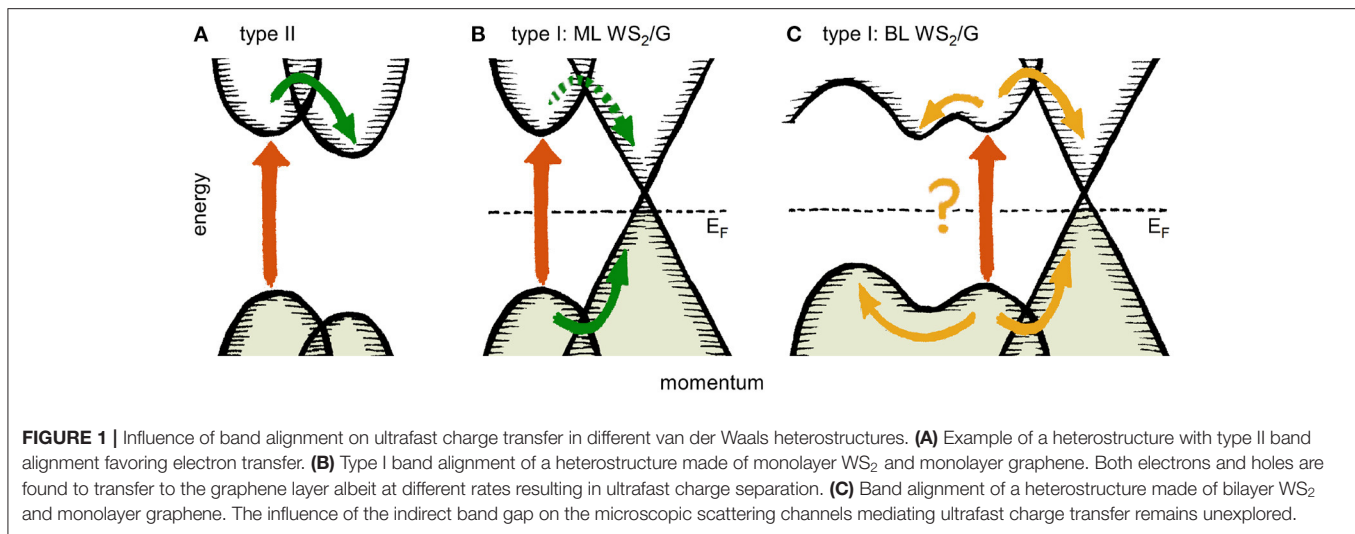
¹ Institute for Experimental and Applied Physics, University of Regensburg, Regensburg, Germany, ² Max Planck Institute for the Structure and Dynamics of Matter, Center for Free Electron Laser Science, Hamburg, Germany, ³ Center for Nanotechnology Innovation at IIT@NEST, Istituto Italiano di Tecnologia, Pisa, Italy, ⁴ National Enterprise for nanoScience and nanoTechnology (NEST), Istituto Nanoscienze, Consiglio Nazionale delle Ricerche (CNR) and Scuola Normale Superiore, Pisa, Italy, ⁵ Graphene Labs, Istituto Italiano di Tecnologia, Genova, Italy, ⁶ Diamond Light Source, Harwell Science and Innovation Campus, Didcot, United Kingdom, ⁷ Central Laser Facility, Science and Technology Facilities Council (STFC) Rutherford Appleton Laboratory, Didcot, United Kingdom, ⁸ Department of Physics and Astronomy, Aarhus University, Aarhus, Denmark

Efficient light harvesting devices need to combine strong absorption in the visible spectral range with efficient ultrafast charge separation. These features commonly occur in novel ultimately thin van der Waals heterostructures with type II band alignment. Recently, ultrafast charge separation was also observed in monolayer WS₂/graphene heterostructures with type I band alignment. Here we use time- and angle-resolved photoemission spectroscopy to show that ultrafast charge separation also occurs at the interface between bilayer WS₂ and graphene indicating that the indirect band gap of bilayer WS₂ does not affect the charge transfer to the graphene layer. The microscopic insights gained in the present study will turn out to be useful for the design of novel optoelectronic devices.

Keywords: TMD, graphene, van der Waals heterostructures, tr-ARPES, ultrafast charge transfer, photovoltaics

1. INTRODUCTION

Solar energy conversion plays an important role in satisfying mankind's ever-increasing energy usage in an environmentally friendly way. Despite several decades of optimization Silicon solar cells still lack efficiency. On the other hand, highly efficient III-V multijunction solar cells are expensive and not sustainable [1, 2]. Recently, van der Waals (vdW) heterostructures made of different monolayer (ML) transition metal dichalcogenides (TMDs) have emerged as a promising new solar cell platform due to their strong excitonic absorption in the visible spectral range [3, 4] followed by efficient ultrafast charge separation due to type II band alignment [5–10] (see **Figure 1A**). Interestingly, ultrafast charge separation was also found to occur in ML WS₂/graphene heterostructures despite the type I band alignment [11–13] (see **Figure 1B**). These heterostructures combine the benefits of a direct gap semiconductor with strong spin-orbit coupling [14, 15] and a semimetal with high-mobility carriers and long spin lifetimes [16] with great potential for novel optoelectronic and optospintronic applications [17].



One simple way to improve the efficiency of WS₂/graphene-based light harvesting devices might be to enhance the thickness and therefore the absorption of the WS₂ layer [18–20]. It is not *a priori* clear, however, if ultrafast charge separation survives when direct-gap monolayer WS₂ is replaced by thicker WS₂ layers with an indirect band gap (**Figure 1C**). In this work we address this issue by exciting carriers across the direct gap at the *K*-point of BL WS₂ in an epitaxial BL WS₂/graphene heterostructure on SiC(0001) and tracing the relaxation of the photogenerated electron-hole pairs as a function of time, energy, and momentum using time- and angle-resolved photoemission spectroscopy (tr-ARPES). We find that photoexcited holes in BL WS₂ are transferred to the graphene layer within 100 fs. The photoexcited electrons are found to remain in the conduction band of BL WS₂ for 420 fs resulting in the formation of a charge separated transient state with a lifetime of 770 fs. These timescales are consistent with the microscopic charge transfer model recently proposed for ML WS₂/graphene heterostructures [13] indicating that also in the case of BL WS₂ on graphene the timescale for charge separation is determined by direct tunneling at the points in the Brillouin zone where WS₂ and graphene bands intersect.

2. METHODS

2.1. Sample Preparation and Characterization

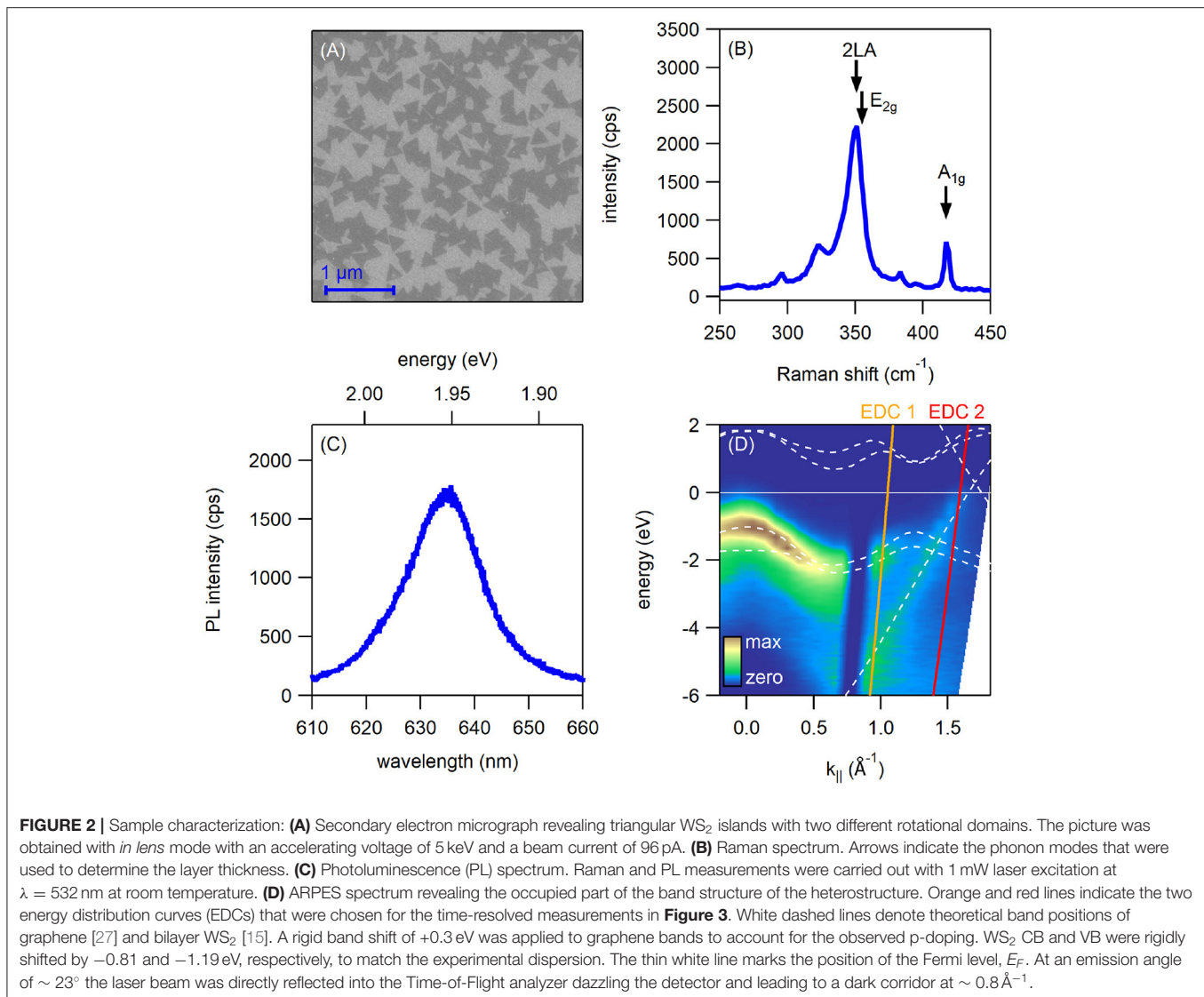
Commercial N-doped 6H-SiC(0001) wafers from SiCrystal GmbH were etched in hydrogen atmosphere and then graphitized by annealing at 1,300°C in argon atmosphere for 8 min [21]. The resulting carbon buffer layer was decoupled from the substrate by hydrogen intercalation at 800°C yielding a completely sp²-hybridized quasi free-standing hole-doped graphene monolayer [22]. WS₂ was grown on top of this graphene layer by low pressure chemical vapor deposition (LPCVD) in a standard hot-wall reactor at a pressure of 1 mbar [23, 24]. Argon served as carrier gas with a flow of 80 sccm. WO₃ and S precursors with a mass ratio of 1:100 were kept at

900 and 120°C, respectively. The WO₃ powder was placed close to the substrate. After growth, the sample was characterized with secondary electron microscopy (SEM), Raman and photoluminescence (PL) spectroscopy, as well angle-resolved photoemission spectroscopy (ARPES).

The SEM picture in **Figure 2A** shows dark triangular WS₂ islands that cover ~ 80% of the graphene layer. The orientation of the triangles reveals the presence of two rotational domains with an angle of 60° between them. From previous low energy electron diffraction measurements on similar samples [11] we deduce that either the ΓK - or the $\Gamma K'$ -direction of the WS₂ islands are aligned with the ΓK -direction of graphene. Further, the topological contrast reveals that ~ 90% of the islands consist of bilayer WS₂. This is consistent with the Raman spectrum shown in **Figure 2B** where the energy of the A_{1g} peak at 417 cm⁻¹ and the intensity ratio between the central peak at 351 cm⁻¹ (2L_A + E_{2g}) and the A_{1g} peak of ~ 6 are indicative of bilayer WS₂ [25]. From the PL spectrum in **Figure 2C** we find a quenched A-exciton resonance at 635 nm (1.95 eV) which confirms the presence of bilayer WS₂ [26]. The ARPES spectrum in **Figure 2D** was taken along the ΓK -direction. We find that the band structure of the heterostructure is a superposition of the band structures of the constituting materials that are indicated by the white dashed lines [15, 27]. The Dirac cone of graphene is found to be hole-doped with the Dirac-point 300 meV above the Fermi level, E_F. As expected for bilayer WS₂ [15] the maximum of the WS₂ valence band is found to be located at the Γ -point.

2.2. Tr-ARPES

Tr-ARPES experiments were performed at the Artemis user facility at the Rutherford Appleton Laboratory in Harwell, UK. We used a Ti:Sa amplifier with a central wavelength of 795 nm, a repetition rate of 1 kHz, 30 fs pulse duration, and 12 mJ pulse energy to generate visible pump and extreme ultraviolet (XUV) probe pulses. Two mJ of output energy were focused into an Argon gas jet for high harmonics generation. A single harmonic at $\hbar\omega_{\text{probe}} = 31.8$ eV was selected with a time-preserving grating



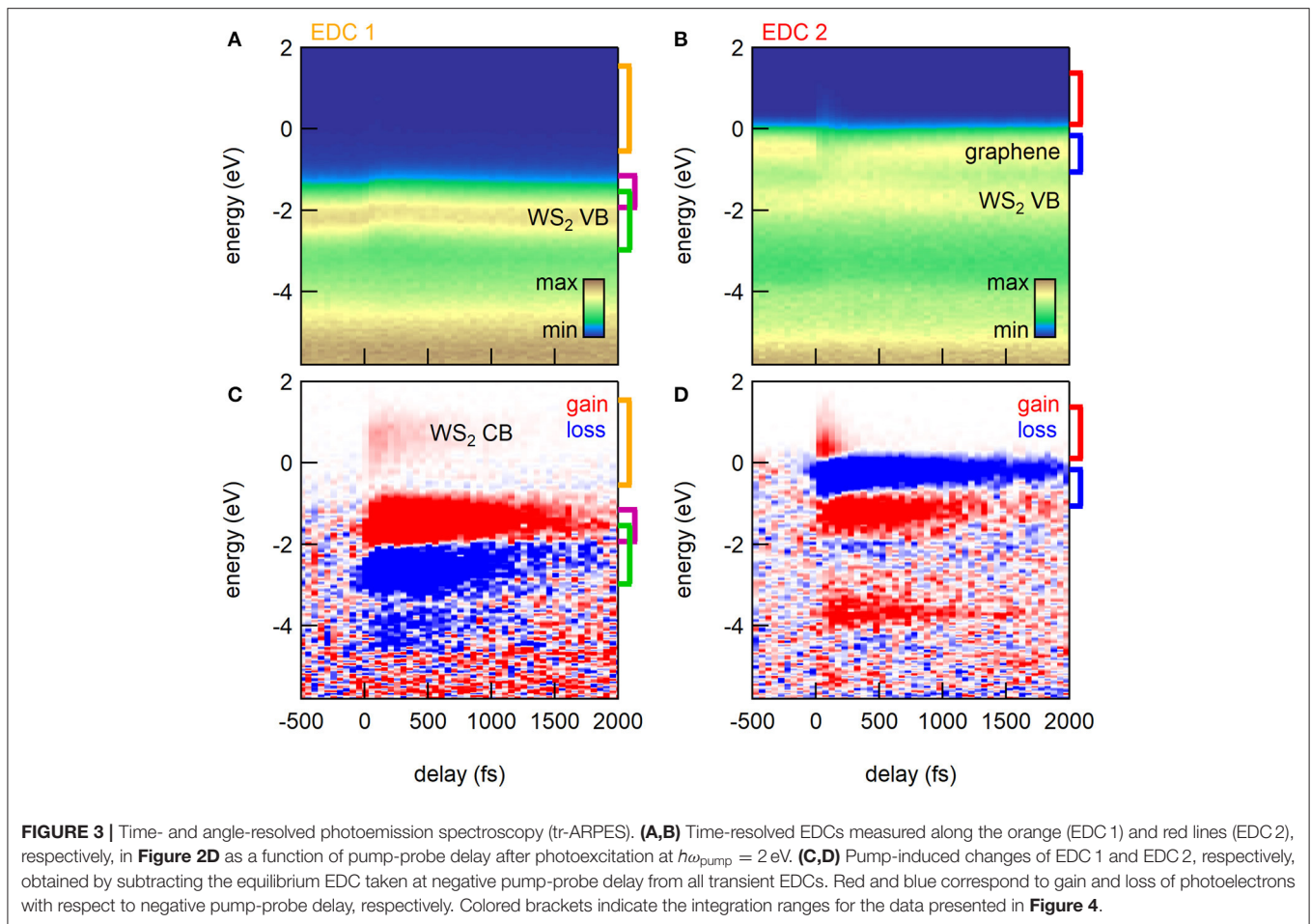
monochromator [28] to be used as the probe. Ten mJ of output power were used to seed an optical parametric amplifier. The signal beam with a photon energy of 1 eV was frequency doubled yielding 2 eV pump pulses matching the A-exciton resonance in WS₂. The kinetic energy of the photoelectrons emitted from the sample by the XUV probe pulse were measured with a home-built Time-of-Flight analyzer with an angular acceptance of 2° [29]. The static ARPES spectrum in **Figure 2D** was obtained by rotating the sample. We measured the energy dependence of the photocurrent at two different emission angles (energy distribution curves, EDCs) as a function of pump-probe delay. The energy and temporal resolution of the experiment were 450 meV and 66 fs, respectively.

3. RESULTS

To investigate ultrafast charge transfer in our BL WS₂/graphene heterostructure we excited carriers across the direct band gap

at the *K*-point of BL WS₂ using 2 eV pump pulses and probed the response of the heterostructure using tr-ARPES. In detail, we investigated the time dependence of two representative energy distributions curves (EDC 1 and EDC 2 in **Figure 2D**) to obtain the population and band structure dynamics of the WS₂ conduction and valence band (CB and VB) and the graphene Dirac cone, respectively. The pump fluence was 6.6 mJ/cm² for EDC 1 (WS₂) and 9.1 mJ/cm² for EDC 2 (graphene).

Figures 3A,B show EDC 1 and EDC 2, respectively, as a function of pump-probe delay. The corresponding pump-induced changes obtained by subtracting the respective EDC at negative pump-probe delay from the transient EDCs are shown in **Figures 3C,D**. Upon arrival of the pump pulse the WS₂ VB is found to shift toward the Fermi level in **Figure 3A**. This up-shift is responsible for the strong gain (red) and loss (blue) signal around -2 eV in **Figure 3C**. **Figure 3C** also reveals a transient gain of photoelectrons in the CB of WS₂ around $+1$ eV following photoexcitation. The graphene π -band in **Figure 3B** is found to



broaden and to shift down which—together with the up-shift of the WS₂ VB at lower energy—produces the gain-loss-gain signal in the energy range between +1 and −2 eV in **Figure 3D**.

To analyze the transient population dynamics of the individual bands we integrated the EDCs in **Figure 3** over the energy range indicated by the colored brackets yielding the pump-probe traces in **Figure 4**. Panel A shows the transient population of the WS₂ VB and CB in green and orange, respectively. The population of the WS₂ VB is found to be unaffected by the photoexcitation within the experimental signal-to-noise ratio. The WS₂ CB on the other hand exhibits a clear gain of electrons. An exponential fit to the data yields a lifetime of the electrons in the WS₂ CB of $\tau = 420 \pm 20$ fs. **Figure 4B** shows the gain above and the loss below the Fermi level in graphene. We find a short-lived gain ($\tau = 97 \pm 3$ fs) and a long-lived loss ($\tau = 840 \pm 30$ fs). The transient up-shift of the WS₂ VB gives rise to a gain of photoelectrons above its equilibrium position that is plotted as a function of pump-probe delay in **Figure 4C**. An exponential fit to the data yields a lifetime of $\tau = 770 \pm 30$ fs.

In agreement with Aeschlimann et al. [11] and Krause et al. [13], we interpret these timescales as follows: The absence of holes in the WS₂ VB together with the short-lived gain in graphene indicates that the photogenerated holes in the WS₂ VB are rapidly (within ~ 100 fs) refilled by electrons from the Dirac

cone. The photoexcited electrons are found to remain in the WS₂ CB for ~ 400 fs, indicating the formation of a charge-separated transient state where the holes reside in the graphene layer and the electrons reside in the WS₂ layer. This charge-separated state is expected to decrease the binding energy of the WS₂ states and to increase the binding energy of the graphene states [11, 13].

Figures 5A,B illustrate the fitting procedure used to determine the transient peak positions of the WS₂ VB and CB and the graphene Dirac cone, respectively. Details are provided in the figure caption. The transient positions of the WS₂ CB and VB are shown in **Figures 5C,D**, respectively. We find that the WS₂ VB shifts up by ~ 110 meV with a lifetime of $\tau = 600 \pm 20$ fs (**Figure 5D**). The transient WS₂ band gap at $k \approx 1.1 \text{ \AA}^{-1}$ obtained by subtracting the transient position of the VB from the transient position of the CB is displayed in **Figure 5E**. An exponential fit yields a transient band gap reduction of ~ 230 meV with a lifetime of $\tau = 140 \pm 40$ fs. Note that the equilibrium gap size of 2.7 eV at $k \approx 1.1 \text{ \AA}^{-1}$ is bigger than the direct band gap at the K-point [13, 30]. In good agreement with Chernikov et al. [31], Liu et al. [32], Ulstrup et al. [33], and Pogna et al. [34], we attribute this band gap renormalization to the presence of photoexcited carriers that screen the Coulomb interaction.

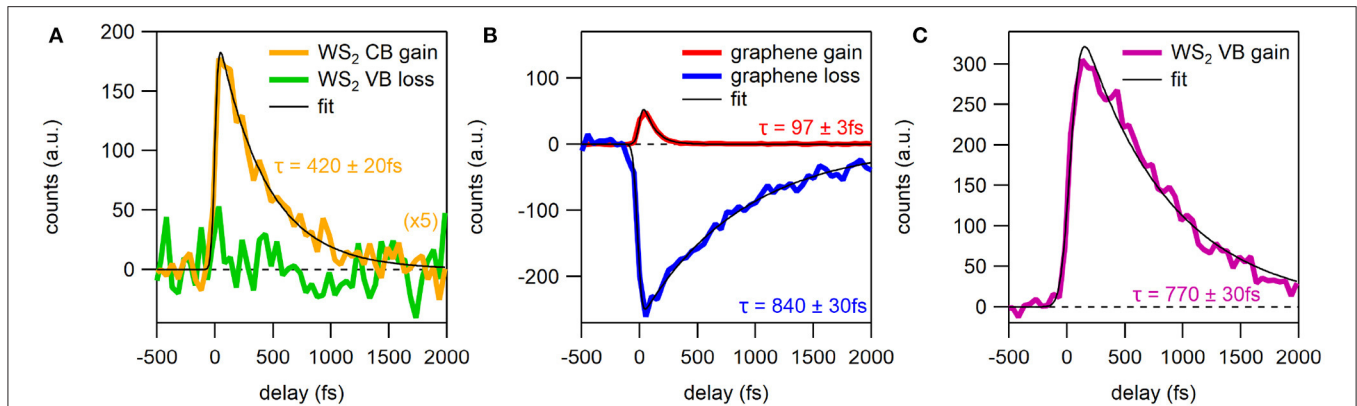


FIGURE 4 | Population dynamics of WS₂ and graphene states. **(A)** Transient occupation of WS₂ conduction band (CB, orange) and valence band (VB, green). The curves were obtained by integrating the photocurrent over the energy range marked by the orange and green brackets in **Figure 3A** for CB and VB, respectively. **(B)** Transient photocarrier dynamics of graphene. The curves were obtained by integrating the photocurrent over the energy range marked by the red and blue brackets in **Figure 3B** corresponding to the gain above E_F and the loss below E_F , respectively. **(C)** Photocurrent integrated over the energy range marked by the purple bracket in **Figure 3C** as a function of pump-probe delay. Black lines are exponential fits to data.

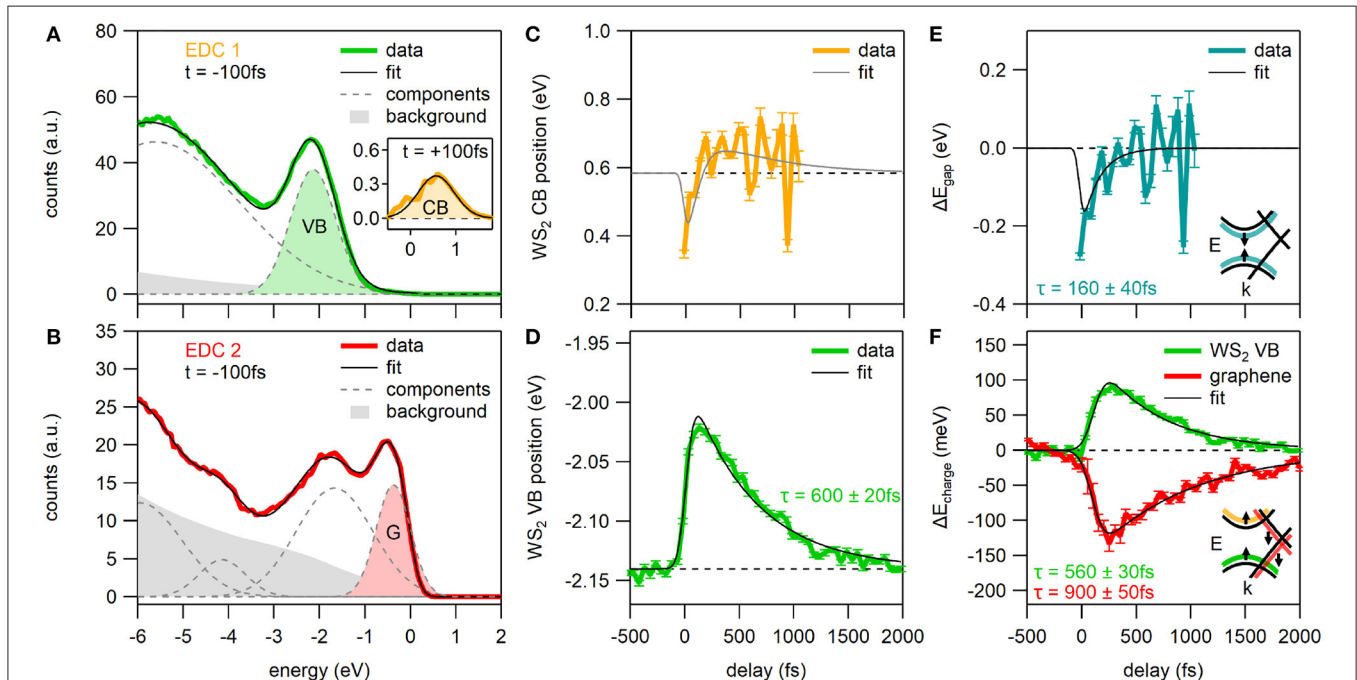
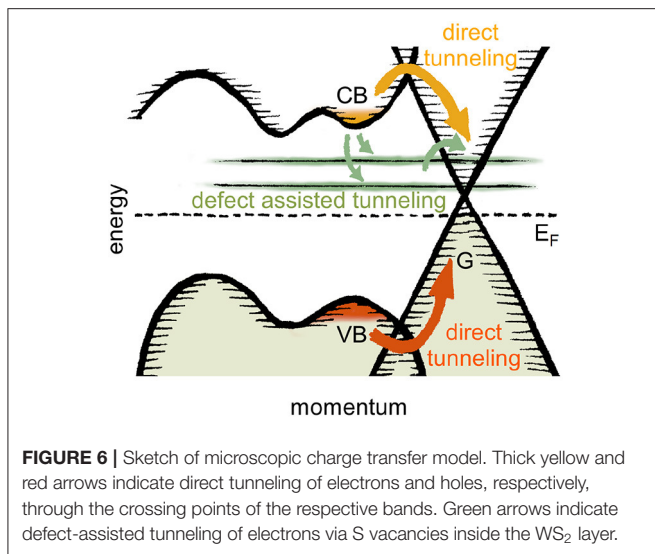


FIGURE 5 | Transient band shifts. **(A)** EDC 1 at negative pump-probe delay together with Gaussian fit. The inset shows the difference EDC 1 at the peak of the pump-probe signal used to fit the binding energy of the WS₂ CB with a single Gaussian. **(B)** EDC 2 at negative pump-probe delay together with Gaussian fit. Fit components and Shirley background are displayed as dashed gray lines and gray-shaded areas, respectively, in **(A,B)**. The peaks that were used to determine the transients peak positions in **(C,D,F)** are shaded in the respective colors in **(A,B)**. **(C)** Transient position of WS₂ CB. **(D)** Transient position of WS₂ VB. **(E)** Transient changes of WS₂ band gap calculated by subtracting **(D)** from **(C)**. **(F)** Charging shifts of WS₂ VB and graphene Dirac cone as a function of pump-probe delay. Black lines are exponential fits to the data.

The transient band gap renormalization results in shifts of the WS₂ VB and CB that are symmetric with respect to the center of the WS₂ band gap (see inset of **Figure 5E**). By subtracting $|\Delta E_{\text{gap}}|/2$ from the transient position of the WS₂ VB we obtain the transient VB shift shown in green in **Figure 5F** that shows a remaining up-shift of ~ 90 meV with a lifetime of $\tau = 560 \pm 30$ fs.

At the same time the π -bands of graphene shown in red in **Figure 5F** shift down by ~ 110 meV with a lifetime of $\tau = 900 \pm 50$ fs. As discussed previously, these shifts are a direct consequence of the transient charge-separated state where excess negative charge on the WS₂ layer decreases the binding energy of the WS₂ states and the corresponding excess positive charge on



the graphene layer increases the binding energy of the graphene states. These charging shifts are sketched in the inset of **Figure 5F**. At this point we are able to attribute the pump-probe signal in **Figure 4C** to the transient up-shift of the WS₂ layer the lifetime of which is linked to the lifetime of the charge-separated state [13]. Also, the dynamics of the WS₂ CB shown in **Figure 5C** can now be explained by the combined effect of band gap renormalization that increases the binding energy of the WS₂ CB on the timescale of the photoexcitation and charging that decreases the binding energy of the WS₂ CB on the timescale of the hole transfer.

All things considered, our data reveals a detailed picture of the ultrafast charge separation following photoexcitation of the WS₂/graphene heterostructure. We find that (1) hole transfer from WS₂ to graphene occurs within ~ 100 fs, (2) photoexcited electrons remain inside the WS₂ CB for ~ 400 fs, and (3) the charge-separated state decays within ~ 800 fs (This number corresponds to the average of the lifetimes of the graphene loss in **Figure 4B**, the WS₂ VB gain in **Figure 4C** and the charging shifts in **Figure 4F**).

4. DISCUSSION

The observed lifetimes for electron and hole transfer are in good agreement with previous tr-ARPES [11, 13] and time-resolved optical techniques [12] on similar WS₂/graphene heterostructures. Next we will discuss if the microscopic model for ultrafast charge separation across the interface between monolayer WS₂ and monolayer graphene [13] also applies to heterostructures made of bilayer WS₂ and monolayer graphene. In this model [13], the timescale for ultrafast charge separation in the heterostructure is determined by direct tunneling of hot carriers from WS₂ to graphene at those points in the Brillouin zone where the respective bands intersect. The associated energy barrier is smaller for holes than for electrons which, combined with a larger tunneling matrix element and a larger scattering phase space, results in hole transfer being faster than electron

transfer. The lifetime of the charge separated state, on the other hand, is determined by defect-assisted tunneling via in-gap states originating from S vacancies inside the WS₂ layer. This decay channel is extremely sensitive to the number of S vacancies in the sample, resulting in lifetimes of the transient charge-separated state between ~ 1 ps in high-quality epitaxial samples [11, 13] and > 1 ns in commercial manually assembled heterostructures [12]. In this model ultrafast charge transfer occurs close to the K-point of WS₂ where the WS₂ VB maximum and CB minimum are located.

It is not *a priori* clear whether this model also applies to heterostructures made of bilayer WS₂ and monolayer graphene because, in this case, the maximum of the WS₂ VB and the minimum of the WS₂ CB are located at Γ and Σ (in between Γ and K), respectively. The observed timescales for hole transfer from WS₂ to graphene within ~ 100 fs and a lifetime of the electrons inside the WS₂ CB at K of ~ 400 fs are perfectly consistent with direct tunneling via band intersections close to the K-point. The lifetime of the charge-separated transient state of ~ 800 fs observed in the present heterostructure is consistent with defect-assisted tunneling via S vacancies in similar high-quality epitaxial samples [11, 13]. Therefore, we conclude that, despite the band structure differences, the microscopic model for ultrafast charge transfer developed for the interface between monolayer WS₂ and monolayer graphene [13] also applies for heterostructures made of bilayer WS₂ and monolayer graphene (see sketch in **Figure 6**).

In summary, we have shown that ultrafast charge separation also occurs at the interface between bilayer WS₂ and monolayer graphene. Together with the enhanced absorption in the visible spectral range compared to monolayer WS₂ our findings provide important insights that will guide the design of novel optoelectronic applications.

DATA AVAILABILITY STATEMENT

The raw data supporting the conclusions of this article will be made available by the authors upon request.

AUTHOR CONTRIBUTIONS

IG, CCa, ES, and CCo organized the project. SF, FF, AR, and CCo prepared the sample. RK, MC-C, SA, SF, FF, AR, YZ, PM, RC, CCa, and IG prepared and conducted the tr-ARPES experiments. RK analyzed the data. RK and IG wrote the manuscript. All authors contributed to manuscript revision, read, and approved the submitted version.

FUNDING

This project has received funding from the European Union's Horizon 2020 research and innovation programme under Grant Agreement No. 654148 Laserlab-Europe, no. 785219 Graphene Core2, and no. 881603 Graphene Core3, from the Deutsche Forschungsgemeinschaft through CRC 925 and CRC 1277 and from UK EPSRC (Grant GR/M50447).

REFERENCES

- Skoplaki E, Palyvos JA. On the temperature dependence of photovoltaic module electrical performance: a review of efficiency/power correlations. *Solar Energy*. (2009) 83:614–24. doi: 10.1016/j.solener.2008.10.008
- King RR, Law DC, Edmondson KM, Fetzer CM, Kinsey GS, Yoon H, et al. Advances in high-efficiency III-V multijunction solar cells. *Adv Optoelectron*. (2007) 2007:1–8. doi: 10.1155/2007/29523
- Wang G, Chernikov A, Glazov MM, Heinz TF, Marie X, Amand T, et al. Colloquium: excitons in atomically thin transition metal dichalcogenides. *Rev Mod Phys*. (2018) 90:021001. doi: 10.1103/RevModPhys.90.021001
- Bernardi M, Palumbo M, Grossman JC. Extraordinary sunlight absorption and one nanometer thick photovoltaics using two-dimensional monolayer materials. *Nano Lett*. (2013) 13:3664–70. doi: 10.1021/nl401544y
- Hong X, Kim J, Shi SF, Zhang Y, Jin C, Sun Y, et al. Ultrafast charge transfer in atomically thin MoS₂/WS₂ heterostructures. *Nat Nanotechnol*. (2014) 9:682–6. doi: 10.1038/nnano.2014.167
- Ceballos F, Bellus MZ, Chiu HY, Zhao H. Ultrafast charge separation and indirect exciton formation in a MoS₂-MoSe₂ van der Waals heterostructure. *ACS Nano*. (2014) 8:12717–24. doi: 10.1021/nn505736z
- Zhu X, Monahan NR, Gong Z, Zhu H, Williams KW, Nelson CA. Charge transfer excitons at van der Waals interfaces. *J Am Chem Soc*. (2015) 137:8313–20. doi: 10.1021/jacs.5b09894
- Chen H, Wen X, Zhang J, Wu T, Gong Y, Zhang X, et al. Ultrafast formation of interlayer hot excitons in atomically thin MoS₂/WS₂ heterostructures. *Nat Commun*. (2016) 7:12512. doi: 10.1038/ncomms12512
- Rivera P, Schaibley JR, Jones AM, Ross JS, Wu S, Aivazian G, et al. Observation of long-lived interlayer excitons in monolayer MoSe₂-WSe₂ heterostructures. *Nat Commun*. (2015) 6:6242. doi: 10.1038/ncomms7242
- Merkel P, Mooshammer F, Steinleitner P, Girnguber A, Lin KQ, Nagler P, et al. Ultrafast transition between exciton phases in van der Waals heterostructures. *Nat Mater*. (2019) 18:691–6. doi: 10.1038/s41563-019-0337-0
- Aeschlimann S, Rossi A, Chávez-Cervantes M, Krause R, Arnoldi B, Stadtmüller B, et al. Direct evidence for efficient ultrafast charge separation in epitaxial WS₂/graphene heterostructures. *Sci Adv*. (2020) 6:eay0761. doi: 10.1126/sciadv.aay0761
- Fu S, Fossé Id, Jia X, Xu J, Yu X, Zhang H, et al. Long-lived charge separation following pump-energy dependent ultrafast charge transfer in graphene/WS₂ heterostructures. *arXiv*. (2020) 200708932. doi: 10.1126/sciadv.abd9061
- Krause R, Aeschlimann S, Chavez-Cervantes M, Perea-Causin R, Brem S, Malic E, et al. Microscopic understanding of ultrafast charge transfer in van-der-Waals heterostructures. *arXiv*. (2020) 201209268.
- Zhu ZY, Cheng YC, Schwingschlögl U. Giant spin-orbit-induced spin splitting in two-dimensional transition-metal dichalcogenide semiconductors. *Phys Rev B*. (2011) 84:153402. doi: 10.1103/PhysRevB.84.153402
- Zeng H, Liu GB, Dai J, Yan Y, Zhu B, He R, et al. Optical signature of symmetry variations and spin-valley coupling in atomically thin tungsten dichalcogenides. *Sci Rep*. (2013) 3:1608. doi: 10.1038/srep01608
- Novoselov KS, Geim AK, Morozov SV, Jiang D, Katsnelson MI, Grigorieva IV, et al. Two-dimensional gas of massless Dirac fermions in graphene. *Nature*. (2005) 438:197–200. doi: 10.1038/nature04233
- Avsar A, Ochoa H, Guinea F, Özyilmaz B, van Wees BJ, Vera-Marun IJ. Colloquium: spintronics in graphene and other two-dimensional materials. *Rev Mod Phys*. (2020) 92:021003. doi: 10.1103/RevModPhys.92.021003
- Zhao W, Ghorannevis Z, Chu L, Toh M, Kloc C, Tan PH, et al. Evolution of electronic structure in atomically thin sheets of WS₂ and WSe₂. *ACS Nano*. (2012) 7:791–7. doi: 10.1021/nn305275h
- Zhu B, Chen X, Cui X. Exciton binding energy of monolayer WS₂. *Sci Rep*. (2015) 5:9218. doi: 10.1038/srep09218
- Raja A, Selig M, Berghäuser G, Yu J, Hill HM, Rigosi AF, et al. Enhancement of exciton-phonon scattering from monolayer to bilayer WS₂. *Nano Lett*. (2018) 18:6135–43. doi: 10.1021/acs.nanolett.8b01793
- Emtsev KV, Bostwick A, Horn K, Jobst J, Kellogg GL, Ley L, et al. Towards wafer-size graphene layers by atmospheric pressure graphitization of silicon carbide. *Nat Mater*. (2009) 8:203–7. doi: 10.1038/nmat2382
- Riedel C, Coletti C, Iwasaki T, Zakharov AA, Starke U. Quasi-free-standing epitaxial graphene on SiC obtained by hydrogen intercalation. *Phys Rev Lett*. (2009) 103:246804. doi: 10.1103/PhysRevLett.103.246804
- Rossi A, Büch H, Rienzo CD, Miseikis V, Convertino D, Al-Temimy A, et al. Scalable synthesis of WS₂ on graphene and h-BN: an all-2D platform for light-matter transduction. *2D Mater*. (2016) 3:031013. doi: 10.1088/2053-1583/3/3/031013
- Forti S, Rossi A, Büch H, Cavallucci T, Bisio F, Sala A, et al. Electronic properties of single-layer tungsten disulfide on epitaxial graphene on silicon carbide. *Nanoscale*. (2017) 9:16412–9. doi: 10.1039/C7NR05495E
- Berkdemir A, Gutiérrez HR, Botello-Méndez AR, Perea-López N, Elías AL, Chia CI, et al. Identification of individual and few layers of WS₂ using Raman Spectroscopy. *Sci Rep*. (2013) 3:1755. doi: 10.1038/srep01755
- Li Y, Li X, Yu T, Yang G, Chen H, Zhang C, et al. Accurate identification of layer number for few-layer WS₂ and WSe₂ via spectroscopic study. *Nanotechnology*. (2018) 29:124001. doi: 10.1088/1361-6528/aaa923
- Wallace PR. The band theory of graphite. *Phys Rev*. (1947) 71:622. doi: 10.1103/PhysRev.71.622
- Frassetto F, Bryan W, Cacho C, Turcu E, Springate E, Poletto L. Time-preserving grating monochromator for extreme-ultraviolet ultrashort pulses. *J Phys Conf Ser*. (2013) 425:122006. doi: 10.1088/1742-6596/425/12/122006
- Cacho CM, Vlaic S, Malvestuto M, Ressel B, Seddon EA, Parmigiani F. Absolute spin calibration of an electron spin polarimeter by spin-resolved photoemission from the Au(111) surface states. *Rev Sci Instrum*. (2009) 80:043904. doi: 10.1063/1.3115213
- Chernikov A, Berkelbach TC, Hill HM, Rigosi A, Li Y, Aslan OB, et al. Exciton binding energy and nonhydrogenic rydberg series in monolayer WS₂. *Phys Rev Lett*. (2014) 113:076802. doi: 10.1103/PhysRevLett.113.076802
- Chernikov A, Ruppert C, Hill HM, Rigosi AF, Heinz TF. Population inversion and giant bandgap renormalization in atomically thin WS₂ layers. *Nat Photonics*. (2015) 9:466–70. doi: 10.1038/nphoton.2015.104
- Liu F, Ziffer ME, Hansen KR, Wang J, Zhu X. Direct determination of bandgap renormalization in the photoexcited monolayer MoS₂. *Phys Rev Lett*. (2019) 122:246803. doi: 10.1103/PhysRevLett.122.246803
- Ulstrup S, Cabo AG, Miwa JA, Riley JM, Grønborg SS, Johannsen JC, et al. Ultrafast band structure control of a two-dimensional heterostructure. *ACS Nano*. (2016) 10:6315–22. doi: 10.1021/acsnano.6b02622
- Pogna EAA, Marsili M, Fazio DD, Conte SD, Manzoni C, Sangalli D, et al. Photo-induced bandgap renormalization governs the ultrafast response of single-layer MoS₂. *ACS Nano*. (2016) 10:1182–8. doi: 10.1021/acsnano.5b06488

Conflict of Interest: The authors declare that the research was conducted in the absence of any commercial or financial relationships that could be construed as a potential conflict of interest.

Copyright © 2021 Krause, Chávez-Cervantes, Aeschlimann, Forti, Fabbri, Rossi, Coletti, Cacho, Zhang, Majchrzak, Chapman, Springate and Gierz. This is an open-access article distributed under the terms of the Creative Commons Attribution License (CC BY). The use, distribution or reproduction in other forums is permitted, provided the original author(s) and the copyright owner(s) are credited and that the original publication in this journal is cited, in accordance with accepted academic practice. No use, distribution or reproduction is permitted which does not comply with these terms.